Vol. 556: 59–77, 2016
doi: 10.3354/meps11865

MARINE ECOLOGY PROGRESS SERIES
Mar Ecol Prog Ser

Published September 8

Spatial variation in rates of benthic denitrification and environmental controls in four New Zealand estuaries

Catherine Gongol[1], Candida Savage[1,2,*]

[1]Department of Marine Science, University of Otago, PO Box 56, Dunedin, New Zealand
[2]Department of Biological Sciences, University of Cape Town, Rondebosch, South Africa

ABSTRACT: Denitrification plays a key role in global biogeochemical cycles as the main nitrogen (N) loss process that limits availability of N to primary producers. This study presents the first measurements of sediment denitrification rates for New Zealand estuaries. Spatially explicit rates of direct denitrification (D_w) and coupled nitrification–denitrification (D_n) were quantified using the isotope pairing method in 4 oligotrophic to moderately nutrient-enriched estuaries on the South Island, New Zealand (Avon-Heathcote, Waikouaiti, Tokomairiro, Tautuku). Coupled nitrification–denitrification dominated (>86%), with most sites having low dissolved inorganic nitrogen (DIN) concentrations (<30 µmol l^{-1}). Rates of total denitrification (D_{tot}) and D_n were negatively correlated with percent sand and positively related to oxygen penetration depth (OPD). Surface sediment chlorophyll *a* concentrations and percent carbon (%C) were also identified as significant predictors of D_{tot} and D_n in the single-factor models. By contrast, D_w was the main nitrogen removal process at moderately nutrient-enriched sites and was positively related to DIN concentrations in the water column and negatively correlated with percent sand. OPD and %C were also identified as significant predictors of D_w. While D_w was positively related to DIN concentrations, overall rates of denitrification were not, demonstrating that predictive relationships between N loading and removal are not always possible in oligotrophic estuaries. Our findings demonstrate the importance of grain size as a driver of denitrification rates in estuaries and imply that an increase in fine-grained sediments from land-use intensification may alter rates of N removal in estuaries through complex direct and indirect processes.

KEY WORDS: Denitrification · Estuaries · New Zealand · Nitrogen · Benthic · Sediment grain size · Isotope pairing method · Oxygen flux

INTRODUCTION

Denitrification, the microbial production of dinitrogen gas (N_2) and nitrous oxide (N_2O) from fixed nitrogen, is the dominant biological process that limits bioavailable nitrogen (N) to primary producers and helps control eutrophication in aquatic systems. In conjunction with physical processes including oceanic exchange (Dettmann 2001), denitrification influences nutrient availability and, therefore, productivity of coastal ecosystems. The spatial distribution of denitrification in estuaries is one of the major uncertainties in global estimates of denitrification (Seitzinger et al. 2006). With the exception of some Australian estuaries (e.g. Cook et al. 2004), there is a paucity of data on spatial variation in denitrification rates for southern hemisphere estuaries and no published data for estuaries in New Zealand.

Denitrification occurs when the combined conditions of nitrate availability, low oxygen concentrations and sufficient organic matter are available, i.e. the direct controls of denitrification (Seitzinger et al. 2006). There are also indirect or secondary controls of denitrification: microphytes and macrophytes, macro-

*Corresponding author: candida.savage@otago.ac.nz

faunal bioturbation and bioirrigation, pH, temperature, salinity, hydrogen sulphide (H_2S), substrata type, and freshwater residence time (Cornwell et al. 1999). Due to spatial variation in direct and indirect controls, total denitrification (D_{tot}) rates vary considerably among estuaries, with reported rates ranging from 0 to 1260 µmol N m^{-2} h^{-1} (Usui et al. 2001, Dong et al. 2006). In general, total N inputs explain a major proportion of the variability in total annual denitrification rates among different estuaries; however, most published studies have been conducted in nutrient-enriched aquatic systems (Seitzinger 1988). Moreover, even across an individual estuary, there is variation in rates of denitrification and the relative proportion of direct denitrification or coupled nitrification–denitrification (Dong et al. 2006), making predictive relationships challenging among and across estuaries.

In aquatic sediments, denitrification can be supported by the diffusion of nitrate (NO_3^-) from the overlying water column into the sediment — direct denitrification (D_w). Alternatively, nitrate can be produced from nitrification in oxic regions of the sediment (Rysgaard et al. 1994) that support denitrification, i.e. coupled nitrification–denitrification (D_n) (Vanderborght & Billen 1975). Since the denitrifying bacteria require suboxic (<0.2 mg O_2 l^{-1}) conditions, this form of denitrification can occur at oxic–anoxic interfaces in sediment. Coupled nitrification–denitrification can account for >90% of the denitrification in aquatic ecosystems when water column NO_3^- concentrations are <10 µmol l^{-1} and the bottom water is well oxygenated, while D_w tends to dominate (>80% of the denitrification) at NO_3^- concentrations >60 µmol l^{-1} (Seitzinger et al. 2006). Prevalence of D_n or D_w has implications for ecosystem models as it affects whether nitrate is supplied locally or distally, the response time of denitrification to changing environmental conditions, and whether diffusive or advective processes are dominant controls of denitrification (Seitzinger et al. 2006).

For the first time, we quantify rates and investigate controls of denitrification in New Zealand estuaries. The present study uses 4 New Zealand estuaries as model ecosystems that vary in nutrient load from oligotrophic to moderately nutrient enriched to investigate spatial variation in the rates of benthic denitrification. Using the isotope pairing method, we can differentiate between D_w and D_n and partition the efflux of the gaseous end products (N_2 and N_2O) across estuarine gradients in the 4 study systems to quantify the relative importance of these 2 forms of denitrification. Further, we investigate which physicochemical factors, in combination and individually, best explain variation in the rates of denitrification (D_{tot}, D_w, and D_n) to identify the environmental factors that influence N removal rates in New Zealand estuaries.

MATERIALS AND METHODS

Sampling locations

Four shallow estuaries (Avon-Heathcote, Waikouaiti, Tokomairiro, and Tautuku) located on the east coast of New Zealand's South Island (Fig. 1) were selected to represent a range of catchment land-use

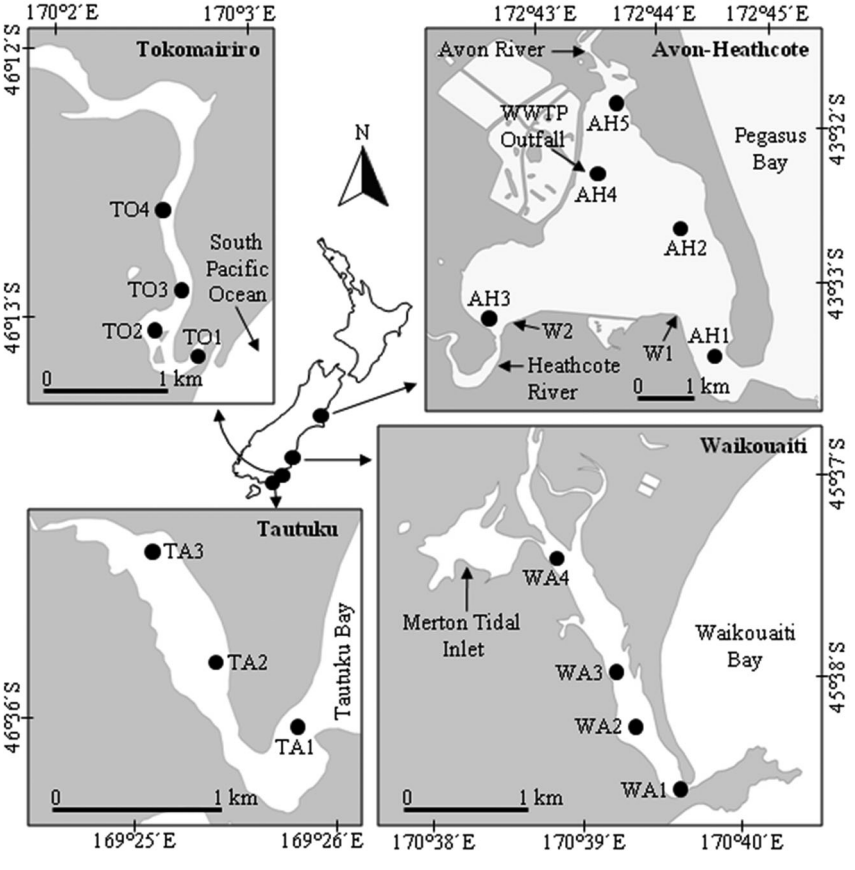

Fig. 1. Study sites within each estuary: Avon-Heathcote, Waikouaiti, Tokomairiro, and Tautuku River estuaries. WWTP: wastewater treatment plant

practices and N loading rates from oligotrophic to moderately nutrient-enriched estuaries. Denitrification rates were quantified at 3–5 sites within each estuary, where the number of sites was based on the size of each estuary. The sites were selected across the salinity gradient to represent the varying environmental conditions from the mouth to the upper estuary.

Avon-Heathcote estuary

The Avon-Heathcote estuary (mean depth: 1.4 m, surface area: 8 km^2) is a triangular-shaped, bar-built estuary (McLay 1976) with a narrow opening to the sea. The estuary catchment is 190 km^2, with the Avon River draining ~85 km^2 from predominantly urban land and the Heathcote River draining ~105 km^2 from rural and urban land. Although the Heathcote River has a greater mean concentration of N than the Avon River, the Avon River contributes more N to the estuary because of the greater annual mean flow (Avon River: 3.2 $m^3 s^{-1}$, Heathcote River: 1.0 $m^3 s^{-1}$). Approximately 80–90% of the N entering the estuary during the study originated from tertiary treated effluent (mainly total nitrogen, TN and ammonia, NH_3) discharged from a wastewater treatment plant (WWTP) (connected population: 323 019, mean flow: 181 000 $m^3 d^{-1}$) twice a day through a single pipeline 1 h before and 3 h after high tide (Bolton-Ritchie & Main 2005). The estuary is moderately nutrient enriched and experiences eutrophication effects, including anaerobic sediment and an overgrowth of opportunistic macroalgae (*Ulva* sp., *Enteromorpha* sp.) in some areas of the estuary (Jones & Marsden 2005). Five subtidal sampling sites (AH1–AH5), which cover a range of sediment types, nutrient concentrations, and salinity levels within the estuary, and 2 water collection sites (W1 and W2) were selected for the study.

Waikouaiti River estuary

The Waikouaiti River estuary (catchment area: 428 km^2, maximum depth: 4 m) is a bar-built estuary (McLay 1976) situated alongside the rural town of Karitane (population: ~345) with a tidal inlet near the head of the estuary. The catchment area is dominated by farming including pastoral dairy, sheep, deer, and beef farming, with fertilizer contributing >70% of the total land-based N inputs (Heggie & Savage 2009). The ocean also contributes N to the estuary (ORC 2000). Macroalgae, including *Bachelotia antillarum* and *Enteromorpha intestinalis*, often bloom in the estuary, which has caused H_2S production in the sediments from the lower and middle reaches of the estuary and a depauperate macrofaunal community (ORC 2000). Four subtidal sampling sites (WA1–WA4), positioned along the length of the lower-mesotrophic estuary, were selected for the study.

Tokomairiro River estuary

The Tokomairiro River estuary (catchment area: 397 km^2, maximum depth: 2 m) is a drowned river estuary (McLay 1976). The catchment comprises ~20% exotic plantation forestry (mainly *Pinus radiata*) and pastoral dairy farming occurs along the banks of the lower Tokomairiro River and estuary. During the study, secondary treated effluent was being discharged from a WWTP into the Tokomairiro River ~20 km upstream of the estuary mouth (connected population: 1887, typical dry weather flow: 600–900 $m^3 d^{-1}$). A textiles factory also likely contributes increased levels of heavy metals, NH_3 and phosphorus (P) in the Tokomairiro River. Four subtidal sampling sites (TO1–TO4) along the length of the oligotrophic estuary were selected for the study.

Tautuku River estuary

The Tautuku River estuary (catchment area: 63 km^2, maximum depth: 2 m) is a bar-built estuary (McLay 1976) fed by the Tautuku and Fleming Rivers. Pristine saltmarsh communities are located adjacent to the oligotrophic estuary. Despite early (1901–1911) modification from logging, there is high diversity of terrestrial species and ~98% of the catchment area today consists of regenerated native forest. Negligible volumes of sewage intermittently enter the estuary from an education center that pumps ~20 $m^3 d^{-1}$ wastewater into a tributary of the Fleming River that drains into the estuary. Three subtidal sampling sites (TA1–TA3) were selected for the study.

Sampling and physicochemical analyses

Each site within the 4 estuaries was sampled in austral spring between August and October 2008 for oxygen data and between September and November

2008 for denitrification rate measurements. Measurements of oxygen were done 1 or 2 wk in advance at each site to provide the information needed to support the denitrification measurements. Sampling was timed to coincide with reasonably elevated water column dissolved inorganic nitrogen (DIN) concentrations following winter rains and before macroalgal blooms assimilate inorganic N from the water column. All sites within a single estuary were sampled at low tide during the same week for oxygen or denitrification and, whenever possible, samples were collected during the morning or early afternoon to minimize any variation in sediment oxygen levels associated with diurnal benthic diatom migration. At each site, a 1.5 × 1.5 m quadrat was randomly positioned and within this area 6 (oxygen) or 15 (denitrification) transparent acrylic cores (8.4 cm internal diameter, 30 cm length) were pushed ~13 cm deep into the sediment. Water (80 l) was also collected on the same day from each site and used with the corresponding sediment cores for each incubation. The exception was water from the Avon-Heathcote estuary, which was collected at high tide at W1 for sites AH1 and AH2 and at W2 for sites AH3, AH4, and AH5 to capture the WWTP discharge. The sediment cores and water were kept in the dark and maintained at *in situ* temperature (±1.0°C) until delivery to the laboratory.

Water column pH, salinity, and temperature were measured, and 3 water samples from each site were filtered (0.45 µm glass microfiber filter) and analyzed for ammonium (NH_4^+) and combined nitrate and nitrite (NO_x^-) on a Lachat Instruments Quickchem 8000 flow injection autoanalyser to quantify water column nutrient concentrations.

Sediment characteristics were measured in triplicate from surface samples (0–2 cm) at each site. The percentage dry weight (DW) of the mud (<0.063 mm) and sand (0.063–2 mm) fractions were determined using the pipette method (Lewis & McConchie 1994). Sediment organic carbon content was measured as mass loss-on-ignition (550°C for 6 h) and porosity was calculated from weight and volume measurements on wet and dry (105°C for 48 h) samples. The chlorophyll *a* (chl *a*) concentration was calculated after extraction of photosynthetic pigments from 5 ± 0.1 g freeze-dried sediment, which were extracted in 10 ml of 90% v/v ethanol by boiling for 2 min and maintaining at room temperature in the dark for 15 h. The supernatant was filtered (Whatman GF/F), and absorbances of the extract were measured at 665 and 750 nm before and after acidification on a UV-1700 PharmaSpec Shimadzu spectrometer.

Pre-incubation

Light was excluded from the sides of the sediment cores using black polythene. The cores were randomly assigned to replicate tanks, where they were immersed in aerated and circulating (300 l h^{-1}) site water. The constant temperature (CT) laboratory was maintained at the mean water temperature for the sampling month (±1.0°C), averaged over a 17 yr period (1989–2005) for Avon-Heathcote (12.1°C) sites, and 13 yr (1995–2007) for the Waikouaiti (12.1°C) and Tokomairiro (14.0°C) sites. Because water temperature records were unavailable for the Tautuku estuary, the CT room for samples from this estuary was maintained at the temperature (±1.0°C) recorded in the field on the first day of sampling (13.2°C). Accordingly, incubations for all sites were performed at 12–14°C.

Overhead illumination in the laboratory was set to a total light intensity of 150 µmol quanta m^{-2} s^{-1} to mimic *in situ* conditions for the shallow subtidal sediments. The laboratory light intensity was based on light measurements made during sampling at the sediment surface (at least 5 readings per site) using a LI-COR LI-185 B quantum photometer and averaged across all 16 sites. In the laboratory, the lights were turned off at sunset and the cores were allowed to equilibrate in the dark overnight. The next morning the lights were turned on at sunrise and the sediment cores were illuminated for 2 h prior to the start of the oxygen and denitrification measurements.

Whole-core sediment oxygen demand

The total flux of dissolved oxygen across the sediment–water interface was determined by closing 3 cores with gastight lids and measuring the change in oxygen concentration in the water column over 4 h. The water column in each chamber was stirred (at 60 rpm, which prevented sediment resuspension) with a motor-driven magnetic rod. The oxygen concentration in each core was measured at the start of the incubation and every hour thereafter (giving a total of 5 measurements) by inserting a fibre optic oxygen sensor (response time: 30–50 s, detection range: 0.01–40.70 ppm, drift <0.02 ppm d^{-1}) connected to an Ocean Optics USB4000-FL spectrometer, through a port in the lid to a height of 5 cm above the sediment surface. The sensor was equilibrated inside the chamber for 2 min, then the oxygen concentration was measured as the mean of 5 readings recorded 1 min apart. After completing the measure-

ment, the port in the lid was sealed with a rubber stopper, leaving no headspace. The concentration of oxygen in the water column of all cores from all estuaries was 99.3 ± 0.8% air saturation at the beginning of the incubations, and during the incubations did not decrease by >20%.

The oxygen sensor was calibrated at the beginning of the incubation in 100% air-saturated site water and in site water that had been deoxygenated with sodium sulphite. A control core with site water but no sediment was also incubated and measured for oxygen to correct for water column activity. In all cases, water column activity was <2% of benthic activity. At the end of the light incubation the lids were removed and the sediment cores were re-equilibrated with the surrounding tank water for ≥4 h (including 2 h in the dark), then measurements were performed in the dark following the same procedures as for the light measurements.

The total flux (J; µmol O_2 m^{-2} h^{-1}) of dissolved oxygen across the sediment–water interface was calculated by linear regression of the oxygen concentration versus time (α) and by considering the area (A; m^2) of the sediment surface and slight differences in the volume (V; l) of water in each chamber ($J = \alpha \times V/A$) (Glud 2008). Negative values were defined as consumption (benthic uptake of oxygen from the water column into the sediment) and positive values as production (benthic release of oxygen from the sediment into the water column).

Vertical oxygen microelectrode profiles

Vertical concentration profiles of dissolved oxygen in the sediment were measured under dark and illuminated conditions with a Clark-type oxygen sensor (Unisense OX100, tip diameter: 90–110 µm) connected to a picoammeter (Unisense PA2000). Measurements were made every 100 µm (measure period of 3 s) from ~2 mm above the sediment surface through the sediment until the signal remained constant with increasing depth. Three replicate profiles (≥3 cm apart) were measured for each of the 3 remaining cores, giving a total of 9 oxygen profiles per site. During measurement, the cores were submerged in larger aerated tanks with circulating water to ensure that the diffusive sediment boundary layer remained at constant thickness. At sunset, the lights were turned off and the sediment cores were allowed to equilibrate in the dark for 2 h before the dark measurements were performed following the same procedures as the light measurements. The oxygen profiles quantify the oxygen penetration depth (OPD), which is the thickness of the oxic layer in the sediments and the most important redox boundary that influences where sedimentary denitrification can occur.

The depth-integrated rates of oxygen consumption and production were calculated from the measured oxygen concentration profiles using the numerical procedure PROFILE v. 1.0 (Berg 1998). To simplify the mathematical model, we assumed that macrofauna had no effect on solute transport and porosity remained constant with sediment depth. The sediment diffusion coefficient for oxygen (d_s), corrected for tortuosity, was calculated using the equation d_s (cm^2 s^{-1}) = $d_o\varphi^2$ (Ullman & Aller 1982), where φ is the mean (n = 3) porosity (ml H_2O ml^{-1} sediment) of the sediment measured at a depth interval of 0–2 cm, and d_o is the free-water diffusion coefficient (cm^2 s^{-1}) for oxygen, taken from the values listed in a table (Broecker & Peng 1974) and corrected for the experimental temperature using the Stokes–Einstein relation (Li & Gregory 1974). The calculation domain was set between the sediment surface and the OPD, with up to 5 equally spaced zones considered for interpretation. The first boundary condition was the oxygen concentration at the bottom of the domain and the second boundary condition was the oxygen flux at the bottom of the domain. The level of significance (p-value) used to determine the zones was 0.01. Only R^2 values >0.85 were accepted and in most cases the R^2 value was >0.99. Calculated negative values represent the diffusive uptake of oxygen from the water column into the sediment, and positive values represent the diffusive release of oxygen from the sediment into the water column.

Denitrification measurements

Rates of denitrification (D_w and D_n) were measured under illuminated conditions using a modified version of the isotope pairing method (IPM) (Nielsen 1992) and the time-series approach. The time-series method uses multiple cores that are terminated at different time intervals to measure the concentration of N_2 and N_2O gas after increasing incubation times. In our experiments, the 5 cores in each tank were used to calculate the rate of denitrification, with each set of 5 cores per tank representing one replicate measurement. A total of 3 replicate measurements of denitrification were quantified at each of the 16 study sites. The incubation conditions were selected to mimic those of intertidal and shallow subtidal sediments, which dominate in these study estuaries.

After pre-incubation, the water inside each tank was drained to isolate the water column of each core. A sample of water was collected from each core and filtered (0.45 µm GF/F). An aliquot of 45 mmol l^{-1} $^{15}NO_3^-$ solution ($K^{15}NO_3^-$, 99 atom% 15N, Cambridge Isotope Laboratories) was added to the water in each chamber to give a final concentration of 5 µmol l^{-1} for sites AH1, AH2, WA1, WA2, WA3, and WA4, and 10 µmol l^{-1} for all remaining sites. The optimum concentration of $^{15}NO_3^-$ was determined by preliminary concentration series experiments using $^{15}NO_3^-$ concentrations of 5–25 µmol l^{-1} to verify a first-order kinetic relationship for N_2 and N_2O efflux and to ensure uniform mixing of the labelled nitrate with the *in situ* nitrate (Dong et al. 2000). After mixing, a second water sample was collected from each chamber so that the initial $^{14}N/^{15}N$ ratio in the NO_3^- pool could be determined. In all cases, the concentration of $^{15}NO_3^-$ corresponded to 30% or more of the *in situ* NO_x^- concentration. The sediment cores were allowed to equilibrate for 1–3 h after the $^{15}NO_3^-$ addition (to establish a 90% steady state profile of $^{15}NO_3^-$), and the water was gently mixed to evenly distribute the $^{15}NO_3^-$ with unlabelled NO_3^- in the porewater. The equilibration time was determined by a numeric model (Dalsgaard et al. 2000) and the OPD (see above).

The cores were capped to start the incubation period and the accumulation of labelled N_2 and N_2O. During incubations, the water column in each chamber was stirred (at 60 rpm, which prevented sediment resuspension) with a motor-driven magnetic rod to simulate *in situ* diffusive boundary layer conditions and ensure homogeneous mixing. During the incubation, the concentration of dissolved oxygen in the water did not change by more than ±20% of air saturation, ensuring that the laboratory setup replicated *in situ* conditions. One sediment core from each of the 3 tanks was terminated at the start of the incubation period. Then, over 6 h, the remaining cores in each tank were individually terminated at 1.5 h intervals to develop the time series of N_2 and N_2O emissions.

To terminate each core, the sediment porewater was gently mixed with the overlying water so that the labelled N_2 and N_2O were distributed homogeneously within the slurry. The extraction and storage of the gases dissolved in the slurry were sampled according to the methodology of Hamilton & Ostrom (2007). Briefly, a 35 ml sample of water was collected into a 50 ml glass syringe followed by 15 ml of helium (99.999% purity, BOC). The syringes were placed into a temperature-controlled water bath with a mechanical shaker and agitated vigorously for 10 min (ca. 450 motions min^{-1}) to transfer the dissolved N_2 and N_2O into the helium headspaces (Weiss 1970, Weiss & Price 1980). Then, >85% of the headspace gas of each syringe was transferred into a 12 ml pre-evacuated exetainer (Labco).

The exetainers were transported inside 50 ml centrifuge tubes filled with distilled water sparged with helium to the stable isotope facility at the University of California, Davis, USA, where the gas samples were analysed within 3 wk of collection. N_2 and N_2O isotope ratios, $[^{29}N_2]\cdot[^{28}N_2]^{-1}$, $[^{30}N_2]\cdot[^{28}N_2]^{-1}$, $[^{45}N_2O]\cdot[^{44}N_2O]^{-1}$, and $[^{46}N_2O]\cdot[^{44}N_2O]^{-1}$, were measured using a SerCon Cryoprep trace gas concentration system interfaced to a PDZ Europa 20-20 isotope ratio mass spectrometer (SerCon). Denitrification rates were calculated according to the equations in Table 1 of Dong et al. (2006).

Macrofauna

The macrofauna in each core were recovered by wet sieving using a 0.5 mm mesh and the fauna were preserved in buffered 10% v/v formalin. As the primary objective of this study was to determine denitrification rates in relation to physicochemical gradients and because of the extensive time and taxonomic expertise needed to identify benthos, the macrofauna from the 5 cores in Tank 1 were sorted and identified (these cores made up the first replicate denitrification rate for each sampling site). Therefore, the macrofauna were correlated against the denitrification measurement from Tank 1 only and not included in the overall distance-based linear models, which included all the environmental parameters (see below). In total, 80 cores (5 from each of the 16 sampling sites) were analysed for benthic fauna. Macrofauna were identified to class level, but the most abundant fauna were identified to species level when possible. Biomass was measured as the wet weight after blotting on lint-free paper and air drying for 5 min.

Statistical analysis

Statistical analyses were performed using the permutational multivariate analysis of variance (PERMANOVA) add-on of PRIMER v.6 (Anderson et al. 2008). PERMANOVA is a permutation approach based on resemblance matrices. A nested 2-factor PERMANOVA was used to test for differences in denitrification rates (D_{tot}, D_w, and D_n) with estuary as a fixed factor (with 4 levels) and sites as a fixed factor (with 5 levels), nested within estuary. Site was cho-

sen as a fixed factor because sites were deliberately chosen across a salinity gradient within each estuary. The measured rates of denitrification were square-root transformed to improve homogeneity of dispersions prior to PERMANOVA analyses. Pairwise comparisons were done among estuaries and among sites nested within each estuary.

The relationship between denitrification and environmental variables was assessed using distance-based linear models (DistLM) in PERMANOVA+ of PRIMER v.6 (Anderson et al. 2008). DistLM is a multiple regression routine where a resemblance matrix (in this case Euclidean distance) is regressed against a set of explanatory variables. Prior to analyses, the measured rates of denitrification were square-root transformed, and explanatory data were transformed when necessary to improve normality. Nutrient concentrations (ammonia, nitrate) were log transformed, chl *a* concentration and %C were square-root transformed, while OPD and grain size were left untransformed. Draftsman plots were used to check for skewness and multi-collinearity in the predictor variables. Variables that were highly correlated with other variables (Pearson's $r > 0.85$) were removed to maximise parsimony of the models. Percent sand covaried with %mud and because %sand had a lower p-value, %sand was used in the analyses to represent sediment grain size. Similarly, sediment oxygen measurements measured in the dark (OPD_{dark}) covaried with the oxygen readings in the light (OPD_{light}), and because denitrification rates were measured under illuminated conditions, the oxygen measurements conducted in the light were used in the models. Similarly, OPD was a better predictor variable than whole-core oxygen flux measurements and hence OPD was retained in the analyses. The final DistLMs were run with 7 predictor variables: water column ammonium concentration (NH_4), nitrate concentration (NO_3), surface sediment (0–2 cm) porosity, %C, and chl *a*, %sand, and OPD measured under illuminated conditions.

The relationship between rates of denitrification and physicochemical explanatory variables was assessed using the 3 replicates from each of the 16 study sites across the 4 estuaries (total n = 48) separately for (1) D_{tot}, (2) D_w, and (3) D_n. Marginal tests in the DistLM routine were used to assess which variables alone explained a significant amount of variation in the denitrification data, ignoring all other variables. In addition, the 'best' selection procedure in DistLM was used to assess the model that uses the best combination of all explanatory variables to explain the greatest amount of variation in the denitrification data based on the corrected Akaike information criterion (AICc). AICc values indicate the goodness of a model fit to the data, whereby models with the lowest AICc are considered the most parsimonious. We calculated the Akaike weights (w_i) of all candidate models within 3 points of the most parsimonious model ($\Delta_i < 3$) and which were included in the 95% confidence set of best-ranked regression models; this provides a measure of uncertainty in model selection (Symonds & Moussalli 2011). The w_i were also used to estimate the relative importance of each predictor variable by adding the w_i of all the models that contained that predictor. The predictors that consistently occur in the most likely models have a w_i close to 1, whereas variables that are absent from or only present in poorly fitting models approximate 0 (Symonds & Moussalli 2011).

To compare macrofaunal communities among sites and estuaries, a Bray-Curtis similarity matrix was calculated on the fourth-root transformed class-level macrobenthic data from the 80 cores that were sorted and identified, and a principal coordinate analysis (PCA) was run.

To assess how much of the variation in denitrification rates was explained by macrofauna, linear regressions were performed between measured rates of denitrification (D_{tot}, D_w, and D_n) from Tank 1 and macrofaunal abundance and biomass from these same cores for which fauna were identified. Because the first 5 cores in Tank 1 were used to calculate the first replicate rate of denitrification according to the established IPM method, the fauna from these 5 cores were combined so that macrofauna abundance and biomass is expressed per 280 cm^2.

RESULTS

Characteristics of the sampling sites

Nutrient concentrations were greatest in the Avon-Heathcote estuary, intermediate at Tautuku estuary and lowest in the Waikouaiti and Tokomairiro estuaries (Table 1). DIN was <30 µmol l^{-1} at most sites, except the upstream sites (AH3, AH4, and AH5) near the WWTP in Avon-Heathcote, where DIN concentrations were between 68 and 140 µmol l^{-1} and NH_4^+ was the dominant form of inorganic N. NH_4^+ and NO_x^- concentrations were approximately equal at all sites in the Waikouaiti and Tokomairiro estuaries. In Tautuku estuary, the NO_x^- concentration was 2–3 times higher than that of NH_4^+. The Tautuku River estuary had the lowest water column pH, ranging

Table 1. Water column and sediment characteristics of the sampling sites at the 4 study estuaries. Data represent means ± SE, n = 3. DW: dry weight; chl *a*: chlorophyll *a*; OPD: oxygen penetration depth

Site	Water column (bottom 0.5 m)				Sediment (top 2 cm)				Sediment
	pH	Salinity (psu)	NH_4^+ (µmol l^{-1})	NO_x^- (µmol l^{-1})	Particle size <0.063 mm (% DW)	Organic carbon (% DW)	Porosity (ml H_2O ml^{-1} sed.)	Chl *a* (µg g^{-1} DW)	OPD_{light} (mm)
Avon-Heathcote									
AH1	8.7	37	11.1±0.5	7.7±0.5	2.1±0.1	1.2±0.0	0.22±0.08	0.1±0.1	7.5±0.8
AH2	8.7	35	7.6±0.8	5.8±1.0	13.1±0.4	1.5±0.0	0.36±0.03	5.7±0.4	3.8±0.8
AH3	8.3	32	45.5±0.9	27.4±0.7	45.4±2.2	2.9±0.1	0.40±0.02	3.3±0.1	3.0±0.8
AH4	8.4	29	39.4±1.4	28.5±1.5	10.7±0.4	1.6±0.0	0.22±0.03	2.2±0.4	3.1±0.7
AH5	8.6	25	113.4±4.9	27.0±2.2	21.7±0.2	1.5±0.1	0.27±0.06	2.2±0.2	3.9±0.8
Waikouaiti									
WA1	8.6	20	1.0±0.4	0.4±0.2	2.3±0.2	0.9±0.0	0.34±0.01	2.2±0.2	7.5±1.1
WA2	8.9	26	1.7±0.5	0.7±0.1	5.6±0.6	1.5±0.1	0.36±0.00	7.4±0.5	6.4±0.8
WA3	8.5	35	1.3±0.5	0.5±0.2	8.4±0.8	1.7±0.2	0.43±0.05	5.9±0.6	4.0±1.0
WA4	8.4	20	0.6±0.3	0.3±0.1	2.2±0.1	1.3±0.0	0.43±0.02	3.3±0.5	5.9±0.8
Tokomairiro									
TO1	8.5	35	1.7±0.3	3.7±0.3	1.5±0.1	0.4±0.0	0.37±0.02	2.4±0.3	9.6±0.7
TO2	8.7	30	2.1±0.3	1.8±0.1	13.4±0.1	1.6±0.1	0.36±0.02	6.6±0.8	9.6±1.0
TO3	8.6	25	1.8±0.1	2.0±0.1	12.2±0.7	1.2±0.1	0.26±0.04	7.3±1.3	8.3±0.7
TO4	8.8	18	1.8±0.4	0.5±0.2	44.2±1.0	3.2±0.0	0.50±0.03	10.5±0.2	8.3±0.7
Tautuku									
TA1	8.2	14	3.7±0.5	6.1±1.2	1.5±0.2	0.9±0.0	0.24±0.03	0.5±0.0	8.5±0.9
TA2	7.7	5	3.6±0.3	12.9±2.2	23.3±0.3	2.6±0.0	0.41±0.01	11.4±1.5	6.4±1.0
TA3	7.5	0	3.2±0.7	13.8±0.6	32.1±1.6	3.4±0.3	0.39±0.03	8.0±1.1	4.1±1.0

from 7.5 at the upstream site (TA3) to 8.2 at the mouth (TA1). Salinities in the water column were generally lower in the upstream sites and higher at the mouth sites, except at the Waikouaiti River estuary, where there was no consistent downstream trend in salinity.

The sediment in the Tokomairiro and Tautuku estuaries was sandy at the mouth and muddy at the upstream sites. In contrast, the sediment was sandy at all 4 sites in Waikouaiti. In Avon-Heathcote, the sediment was sandy at the mouth (AH1), muddy at AH3, and muddy sand at the remaining sites (AH2, AH4, and AH5). In the Waikouaiti, Tokomairiro and Tautuku River estuaries, the organic carbon content was lowest at the mouth and highest at the upstream sites. The sediment porosity at all sites ranged from 0.50 ml H_2O ml^{-1} sediment (at TO4) to 0.22 ml H_2O ml^{-1} sediment (at AH1 and AH4). Sediment chl *a* content was generally low (on average, 4.9 µg g^{-1} DW across all sites), with no clear trends across the estuaries. Chl *a* concentrations were lowest at AH1 (0.1 µg g^{-1} DW) and highest at TA2 (11.4 µg g^{-1} DW) and TO4 (10.5 µg g^{-1} DW).

OPD in the sediment measured under illuminated conditions varied between 3.0 mm at AH3 and 9.6 mm at TO1 and TO2 (Table 1). At Avon-Heathcote, the mean OPD was 3.5 mm, except at the mouth site (AH1, 7.5 mm). Similarly, OPD was 7.5 mm at the mouth site at Waikouaiti but decreased to an average of 5.4 mm across the other sites. Sediments at the Tokomairiro estuary mouth had an average OPD of 9.0 mm. There was a clear gradient in decreasing OPD at Tautuku estuary, with an average 8.5 mm measured at the mouth, 6.4 mm at the mid-estuarine site, and 4.1 mm at the upper estuarine site. The OPD was significantly ($p < 0.05$) greater in the light (Table 1) than in the dark only at the mouth and middle estuary sites (mean ± SE OPD in dark in parentheses): AH1 (5.7 ± 0.5 mm), AH2 (3.0 ± 0.2 mm), WA2 (5.0 ± 0.3 mm), TO1 (8.5 ± 0.1 mm), TO2 (8.1 ± 0.6 mm), and TA2 (3.9 ± 0.9 mm).

Macrofaunal communities from the 4 study estuaries were separated into 2 major groups along the first axis of the PCA (explaining 51% variance), with Avon-Heathcote and Waikouaiti sites forming one group and the Tokomairiro mouth and Tautuku sites the second group, with similar composition and abundance of macrofaunal classes (Fig. 2). Mouth and upper estuarine sites (Sites 1 and 5) in the Avon-Heathcote and Waikouaiti estuaries were dominated by bivalves, with gastropods also recorded in relatively high numbers. In Waikouaiti, the dominant bivalve was the suspension-feeding clam *Austro-*

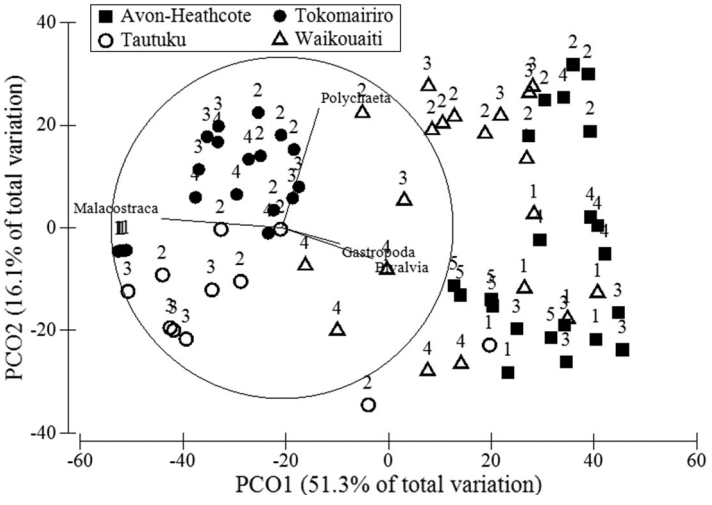

Fig. 2. Principal coordinate analysis (PCA) of the macrofaunal community abundance data at the study sites of the 4 estuaries. The PCA is based on fourth-root transformed macrofauna classes using the Bray-Curtis index of similarity. The numbers (1–5) represent the sites, where 1 is the mouth site of each estuary and 4 and 5 are upper estuarine sites. Dominant macrofaunal classes are shown in the vectors

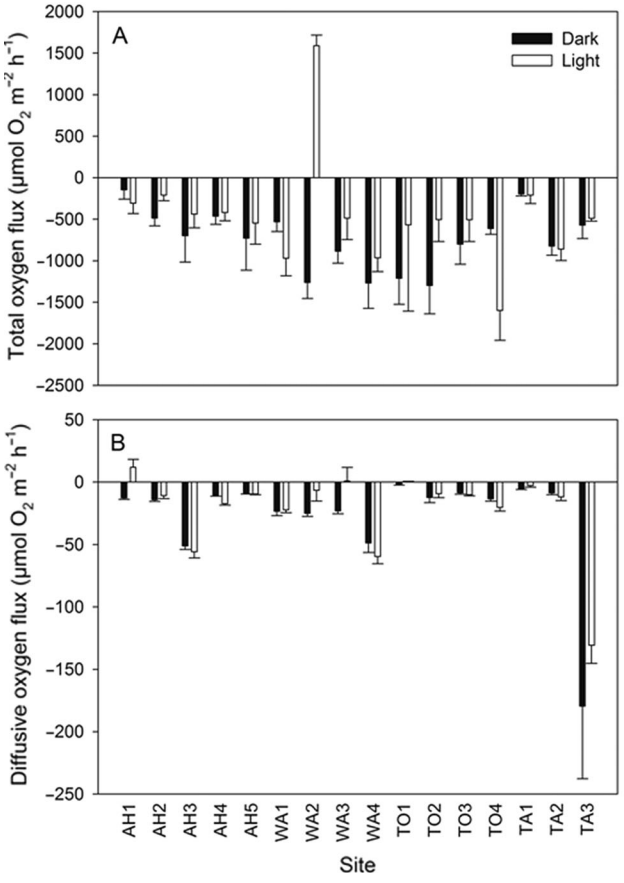

Fig. 3. Fluxes of dissolved oxygen measured across the sediment–water interface under dark and illuminated conditions using (A) benthic chamber incubations (data represent means ± SE; n = 3) and (B) microelectrode profiles (data represent means ± SE; n = 9). Negative values represent consumption and positive values represent production. Note the different scales on the *y*-axes

venus stutchburyi, while at Avon-Heathcote the surface-deposit-feeding bivalve *Macomona liliana* occurred in addition to *A. stutchburyi*. At mid-estuarine sites (2, 3), polychaetes were relatively more abundant, with Spionidae the most common polychaete family, and Orbiniidae, Sabellidae, and Nereididae also found in reasonably high numbers in these 2 estuaries. By contrast, the macrofauna community at the Tokomairiro and Tautuku River estuaries was dominated by amphipods (class Malacostraca), particularly at Tokomairiro, where up to 100–200 juvenile amphipods were counted in some cores. Polychaeta belonging to the family Spionidae were also abundant, while bivalves were present but occurred in low numbers at these 2 estuaries. Mouth sites at all study estuaries generally had very low numbers of macrofauna.

Total and diffusive oxygen fluxes

The diffusive oxygen exchange rate was generally <10% of the total sediment oxygen exchange rate (Fig. 3). There was no significant ($p > 0.05$) relationship between the total flux of oxygen across the sediment–water interface and the diffusive oxygen flux measured in the light or dark at all sites in the 4 estuaries. Oxygen fluxes were generally similar in both light- and dark-incubated sediment. Under illuminated conditions, oxygen production occurred only at a few sites. WA2 was the only site where the total flux of oxygen measured in the light (1588 ± 128 µmol m^{-2} h^{-1}) was significantly greater (i.e. production versus consumption) than the total flux of oxygen measured in the dark (–1261 ± 192 µmol m^{-2} h^{-1}; paired-samples *t*-test $t_2 = -29$, $p = 0.001$). The diffusive flux of oxygen was significantly greater in the light than in the dark only at the mouth sites AH1 ($t_8 = -3.5$, $p = 0.008$), TO1 ($t_8 = -7.8$, $p < 0.001$), and TA1 ($t_8 = -2.7$, $p = 0.025$). At AH4, oxygen consumption occurred under both dark and light experimental conditions, but the consumption in the light (–17.3 ±1.2 µmol m^{-2} h^{-1}) was significantly greater than the consumption (–10.4 ± 0.84 µmol m^{-2} h^{-1}) in the dark ($t_8 = 5.065$, $p = 0.001$). The results of a Kruskal-Wallis test showed that there was no significant ($p > 0.05$) difference among the 4 estuaries in the mean total or diffusive fluxes of oxygen

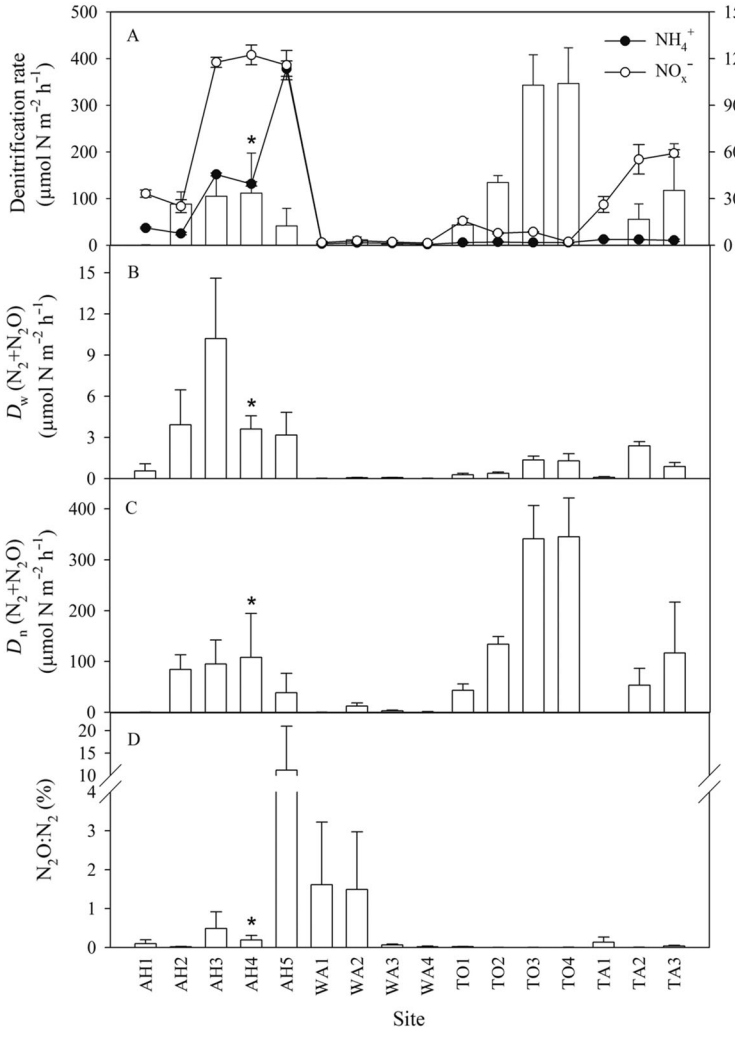

Fig. 4. (A) Mean rates of total denitrification and the *in situ* concentration of NH_4^+ (●) and NO_x^- (○) in the water column, (B) mean rates of N_2 and N_2O production from direct denitrification (D_w), (C) mean rates of N_2 and N_2O production from coupled nitrification–denitrification (D_n), and (D) mean ratio of the rates of N_2O and N_2 production ($N_2O/N_2 \times 100$) at the sites within the 4 study estuaries. Bars indicate SE (n = 3, except where an asterisk is present, in which case n = 2). Note the different scales on the *y*-axes

measured in the dark or light. However, there were some significant ($p < 0.05$) differences in the fluxes of oxygen among sites within individual estuaries.

Rates of denitrification

Rates of denitrification measured in the study estuaries varied from 0.06 ± 0.05 μmol N m^{-2} h^{-1} (at WA1) to 346.6 ± 76.2 μmol N m^{-2} h^{-1} (at TO4) (Fig. 4A). The mean rate of total denitrification was significantly different among estuaries (Table 2). On average, the highest denitrification rates occurred in the Tokomairiro estuary (mean: 216.8 μmol N m^{-2} h^{-1}), the lowest rates occurred in the Waikouaiti estuary (mean: 3.8 μmol N m^{-2} h^{-1}), and moderate rates occurred in the Tautuku (mean: 57.8 μmol N m^{-2} h^{-1}) and Avon-Heathcote (mean: 69.4 μmol N m^{-2} h^{-1}) estuaries. Pairwise tests showed that all the study estuaries were significantly different in rates of total denitrification, except Avon-Heathcote and Tautuku estuaries ($p = 0.40$; Table 2). Similarly, all estuaries were significantly different ($p < 0.05$) from one another in mean rates of D_n and D_w, except Tautuku and Avon-Heathcote. D_n accounted for 86% of the denitrification at all study sites except AH1 (1.84%) and TA1 (0.00%), where total rates of denitrification were low (0.55 ± 0.52 and 0.08 ± 0.05 μmol N m^{-2} h^{-1}, respectively). Rates of D_n were highest at the mouth of the Tokomairiro estuary, especially at TO3 and TO4 (Fig. 4C). By contrast, the highest rate of D_w (10.2 ± 4.4 μmol N m^{-2} h^{-1}) occurred at AH3 and the lowest rate (0 μmol N m^{-2} h^{-1}) occurred at WA4 (Fig. 4B). The rate of N_2O production was much lower than the rate of N_2 production, with the highest rate of N_2O production measured across all sites being 0.19 ± 0.08 μmol N m^{-2} h^{-1} at AH5. The ratio between N_2O:N_2 fluxes ($N_2O/N_2 \times 100$) was highest at AH5 (11.20%; Fig. 4D).

Within each estuary, pairwise tests demonstrated that all sites across the estuary had significantly different ($p > 0.05$) rates of denitrification, with the lowest rates recorded at the mouth sites. In the Avon-Heathcote estuary, the rates of denitrification ranged from 0.55 ± 0.52 μmol N m^{-2} h^{-1} at the mouth site (AH1) to 111.7 ± 85.7 μmol N m^{-2} h^{-1} at the site (AH4) closest to the WWTP outfall. In the Waikouaiti River estuary, denitrification rates ranged from 0.06 ± 0.05 μmol N m^{-2} h^{-1} at the mouth site (WA1) to 12.0 ± 6.1 μmol N m^{-2} h^{-1} at the mid-estuary site (WA2) located adjacent to WA1. The rates of denitrification in the Tokomairiro River estuary ranged from 43.3 ± 12.5 μmol N m^{-2} h^{-1} at the mouth site (TO1) to 346.6 ± 76.2 μmol N m^{-2} h^{-1} at the site (TO4) furthest upstream. In the Tautuku River estuary, the rates of denitrification decreased down the estuary from the upstream site (TA3: 117.7 ± 100.1 μmol N m^{-2} h^{-1}) to the mid-estuarine site (TA2: 55.5 ± 32.9 μmol N m^{-2} h^{-1}) and to the mouth site (TA1: 0.08 ± 0.05 μmol N m^{-2} h^{-1}).

Table 2. Results of nested 2-factor PERMANOVA for differences in rates of total denitrification among estuaries and among sites nested within estuaries. Results of pairwise comparisons for estuaries, where ≠ denotes estuaries that are significantly different in terms of overall denitrification rates, are as follows: Avon-Heathcote ≠ Waikouaiti (p = 0.0006), Avon-Heathcote ≠ Tokomairiro mouth (p = 0.0002), Avon-Heathcote = Tautuku (p = 0.4002), Waikouaiti ≠ Tokomairiro mouth (p = 0.0001), Waikouaiti ≠ Tautuku (p = 0.0246), Tokomairiro mouth ≠ Tautuku (p = 0.001)

Source of variation	df	SS	MS	Pseudo-*F*	p
Estuary	3	960.37	320.12	25.854	0.0001
Site (Estuary)	12	625.7	52.141	4.2111	0.0005
Residual	32	396.22	12.382		
Total	47	1982.3			

Environmental drivers of denitrification

D_{tot} and D_n were strongly correlated with sediment grain size and sediment oxygen conditions, while D_w was correlated with sediment grain size and water column nutrient concentrations. The best models using DistLM explained over 50% of the variation in denitrification rates and included 2 variables: %sand and OPD for D_{tot} and D_n, and %sand and ammonia concentration for D_w (Table 3). There was a 28 to 43% chance that these were the best approximating models for D_{tot} and D_n, respectively (demonstrated by the w_i value; Table 3), with all other candidate models identified within 95% confidence containing these same variables. Similarly, %sand and OPD had the highest w_i for total and coupled nitrification–denitrification when predictors were tested individually (0.881 for D_{tot} and 0.813 for D_n; Table 4), while %sand and ammonia had the highest w_i (0.859) for direct denitrification, indicating that these variables occurred in the most likely models. Denitrification rates were negatively related to %sand, which explained between 29% (D_w) and 43% (D_{tot}, D_n) of the variation in denitrification rates when the variables were considered alone. The marginal tests also identified sediment chl *a* concentration and %C as significant factors that were positively related to D_{tot} and D_n, explaining 23 and 14–16% of the variance, respectively. Rates of total denitrification and D_n were positively correlated with total abundance of macrofauna when considering the data from all 4 estuaries (R^2 = 0.61, p < 0.001; Fig. 5). By contrast, rates of D_w were not significantly related to total abundance of macrofauna (R^2 = 0.02, p = 0.585).

Direct denitrification was significantly (p < 0.0001) positively related to water column nutrient concentrations, with nitrate and ammonia concentrations individually explaining 43 and 37%, respectively, of the variance in spatial differences in D_w (Table 4). In addition to nutrient concentrations and %sand, the

Table 3. The best regression models (95% confidence, i.e. cumulative Akaike's weight [acc. w_i] < 0.95) that explain variance in denitrification when considering all the variables together. The candidate models are identified by the 'best' model selection in the distance-based linear model (DistLM) routine using corrected Akaike's information criterion (AIC_c), with the model with the lowest AIC_c value presented in **bold**. R^2: amount of variance explained; RSS: residual sum of squares; *k*: number of predictor variables included in each model, Δ_i: difference in AIC_c value between each candidate model and the best model; w_i: Akaike weight. %sand: percent sand; %C: percent carbon content; chl *a*: chlorophyll *a*; OPD: oxygen penetration depth

Candidate model	AIC_c	R^2	RSS	*k*	Δ_i	w_i	Acc. w_i
Total denitrification (D_{tot})							
%sand + OPD	**146.36**	**0.554**	**883.69**	**2**	**0**	**0.280**	**0.280**
%sand + OPD + NO_3	147.1	0.569	853.92	3	0.74	0.193	0.473
%sand + OPD + %C	147.64	0.564	863.54	3	1.28	0.147	0.620
%sand + OPD + NH_4	147.78	0.563	865.93	3	1.42	0.137	0.757
%sand + OPD + NO_3 + %C + Chl *a*	147.99	0.606	781.78	5	1.63	0.124	0.881
Coupled nitrification–denitrification (D_n)							
%sand + OPD	**153.1**	**0.512**	**1016.8**	**2**	**0**	**0.428**	**0.428**
%sand + OPD + %C	154.67	0.520	999.78	3	1.57	0.195	0.624
%sand + OPD + NO_3	154.73	0.520	1001	3	1.63	0.190	0.813
Direct denitrification (D_w)							
NH_4 + %sand	**–47.26**	**0.604**	**15.647**	**2**	**0**	**0.315**	**0.315**
NH_4 + %sand + NO_3	–46.49	0.617	15.13	3	0.775	0.214	0.529
NH_4 + %sand + Porosity	–46.21	0.615	15.216	3	1.046	0.187	0.715
NH_4 + %sand + Chl *a*	–45.69	0.610	15.383	3	1.571	0.144	0.859

Table 4. The importance of the explanatory variables as drivers of denitrification based on distance-based linear models (DistLM). The marginal tests assess the amount of variation explained by each predictor variable alone, when ignoring other variables. The proportion of explained variance for each significant variable is presented (*p < 0.05, **p < 0.01, ***p < 0.001). Variables that were not significant (ns) in the marginal tests, but which had an Akaike weight (w_i) >0.5, are listed as they were identified as important in the 'best' models. Variables close to 1 consistently occur in the most likely models. %sand: percent sand; chl *a*: chlorophyll *a*; %C: percent carbon; OPD: oxygen penetration depth; NO_3: nitrate concentration; NH_4: ammonia concentration

Explanatory variable	Marginal tests	Relative importance of variable	Direction of relationship
Total denitrification (D_{tot})			
%sand	0.48***	0.881	Negative
Chl *a*	0.23***	0.124	Positive
%C	0.16**	0.271	Positive
OPD	ns	0.881	Positive
NO_3	ns	0.317	Positive
NH_4	ns	0.137	Positive
Coupled nitrification–denitrification (D_n)			
%sand	0.43***	0.813	Negative
Chl *a*	0.23***	–	Positive
%C	0.14**	0.195	Positive
OPD	ns	0.813	Positive
NO_3	ns	0.190	Positive
Direct denitrification (D_w)			
NO_3	0.43***	0.214	Positive
NH_4	0.37***	0.859	Positive
%sand	0.29***	0.859	Negative
OPD	0.23***	–	Positive
%C	0.17**	–	Positive
Porosity	ns	0.187	Positive
Chl *a*	ns	0.144	Positive

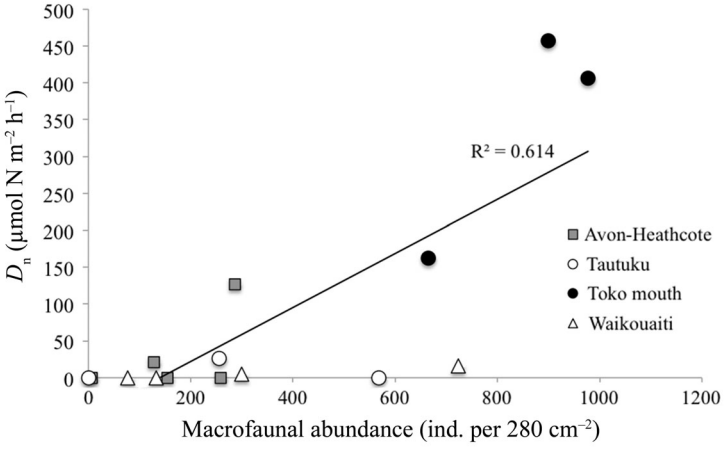

Fig. 5. Linear regression of the rate of coupled nitrification–denitrification (D_n) versus total macrofaunal abundance. Data represent the combined macrofaunal abundance from the 5 cores in Tank 1 and are therefore expressed per 280 cm^2. The rate of D_n from the same cores where macrofauna were identified is presented

marginal tests also identified OPD (23% variance, $p < 0.001$) and %C (17% variance, $p < 0.01$) as significant variables when considered alone. All factors were positively related to rates of denitrification except %sand, which was negatively related to N removal rates.

DISCUSSION

This study presents the first measurements of denitrification using multiple sites in 4 New Zealand estuaries and adds to the limited data on biogeochemical cycles in southern hemisphere estuaries. The study also offers new knowledge on spatially explicit rates of N removal in oligotrophic estuaries. Denitrification rates in the New Zealand study estuaries varied between 0.1 to 346.6 µmol N m^{-2} h^{-1}, with the highest rates measured in the Tokomairiro River estuary (43–347 µmol N m^{-2} h^{-1}) and the lowest rates (0–12 µmol N m^{-2} h^{-1}) in the Waikouaiti River estuary. These values are within the range of denitrification rates (0–458 µmol N m^{-2} h^{-1}) reported for estuarine systems worldwide where the isotope pairing method was used (Table 5). The different methods available to measure denitrification affect the rates quantified (Groffman et al. 2006), and accordingly it is inappropriate to compare denitrification rates measured with different techniques. The IPM has the advantage of being able to partition D_w and D_n and was therefore selected for the present study because we wanted to understand the relative importance of these two N removal processes using a spatially explicit sampling scheme.

Spatial variation in denitrification across individual estuaries showed inconsistent patterns in downstream N removal rates, with denitrification rates decreasing significantly down the estuary in 2 study estuaries (Tokomairiro and Tautuku), while there was no consistent trend in the Waikouaiti and Avon-Heathcote estuaries. Similarly, the literature reports conflicting results, with either no significant relationship between the rate of denitrification and the location within an estuary (e.g. Seitzinger 1987) or decreases in rates from the head to the mouth sites of estuaries as NO_3^- concentrations were lowered (Dong et al. 2006). Our findings suggest that the intertidal sediments in Tokomairiro and Tautuku effectively attenuate N loads from the head to the mouth of the estuary, while Avon-

Table 5. Rates of denitrification and coupled nitrification–denitrification (D_n) measured using the isotope pairing method in sediment from freshwater, estuarine, and marine environments. NZ: New Zealand

Location	Denitrification rate (μmol N m^{-2} h^{-1})	D_n (% of denitrification)	Source
Northern Baltic Proper	1–12	39–67	Tuominen et al. (1998)
Gulf of Finland, Baltic Sea	4–27	54–95	Tuominen et al. (1998)
Southern Baltic Sea	0–29	>70	Deutsch et al. (2010)
River Colne estuary, England	3–458	0–81	Ogilvie et al. (1997)
River Colne estuary, England	0–6000	0–100	Dong et al. (2000)
River Colne estuary, England	9–422	<10–75	Dong et al. (2006)
Humber estuary, England	0–320	40–70	Dong et al. (2006)
Conwy estuary, England	0–108	30–65	Dong et al. (2006)
Tagus estuary, Portugal	<10–250	55–90	Cabrita & Brotas (2000)
Wadden Sea, Germany	0–17	25–31	Jensen et al. (1996)
North Sea	9–13	95	Lohse et al. (1996)
Kertinge Nor, Denmark	<1–75	20–50	Rysgaard et al. (1995)
Åarhus Bay, Denmark	32–34	90–95	Eyre et al. (2002)
Norsminde Fjord, Denmark	120	100	Eyre et al. (2002)
Norsminde Fjord, Denmark	162–221	16–31	Rysgaard et al. (1993)
Norsminde Fjord, Denmark	87–217	8–27	Risgaard-Petersen et al. (1994)
Salten Å stream, Denmark	4–105	<5–20	Nielsen (1992)
Vallda, Sweden	0–4	70–80	Sundbäck et al. (2000)
Rörtången, Sweden	0–40	57–69	Sundbäck et al. (2000)
Avon-Heathcote estuary, NZ	0–112	2–97	Present study
Waikouaiti River estuary, NZ	0–12	87–99	Present study
Tokomairiro River estuary, NZ	43–347	99	Present study
Tautuku River estuary, NZ	0–118	0–99	Present study

Heathcote had areas of greater N removal at sites closer to the WWTP, which had greater mud content and relatively high DIN concentrations. Spatial variability in N removal rates were also found by Gran and Pitkänen (1999), with lowest rates of sediment denitrification (<1 μmol N m^{-2} h^{-1}) in the inner Neva estuary in the eastern Gulf of Finland, higher rates (2–10 μmol N m^{-2} h^{-1}) downstream in the outer, more organic-rich sediments of the estuary, and the highest rates (30–50 μmol N m^{-2} h^{-1}) in the open gulf, where bioturbating macrofauna were present in high abundances. Multiple factors, including nutrient concentrations, sediment type, and macrofauna, can directly and indirectly influence rates of benthic denitrification across estuaries and make it difficult to predict hotspots of N removal within an estuary. Consequently, we used a multivariate approach to investigate the environmental factors that best explain variance across all estuarine sites (see below). A further complication in predicting N removal hotspots in estuaries is that denitrification can be supported by nitrate either from the water column (D_w) or via nitrification in the sediments (D_n), which has implications for whether advective or diffusive processes dominate N removal in estuaries.

Our study highlights the importance D_n in New Zealand's oligotrophic estuaries. Denitrification was mainly supported by NO_3^- produced via nitrification in the sediments, with rates of D_n 6–355 orders of magnitude greater than rates of D_w (Fig. 4), except at sites AH1 and TA1, which had very low rates of total denitrification. The study estuaries have low nitrate concentrations in the water column (<30 μmol l^{-1}), with even the most eutrophic of the study estuaries (Avon-Heathcote) having extremely low NO_x^- concentrations (6–28 μmol l^{-1}) during sampling. It is thus not surprising that D_n dominated the New Zealand study estuaries, as nitrate concentrations were probably too low to support D_w, in agreement with another study on an unpolluted estuary (Seitzinger 1987). In contrast, N removal in most estuaries in Europe and North America is mainly dominated by D_w (e.g. Colne Estuary, UK: 5–483 μmol l^{-1}, Humber Estuary, UK: 5–306 μmol l^{-1}; Dong et al. 2006). In our study, D_w was proportionally more important as a N removal mechanism at sites with greater water column N concentrations, including the middle and upstream sites in the Avon-Heathcote estuary, where DIN exceeded 68 μmol l^{-1}. Our findings therefore support the hypothesis that the water column is generally the dominant source of NO_3^- for denitrification only at NO_3^- concentrations >60 μmol l^{-1} (Seitzinger et al. 2006). Further, water column nutrient concentrations were identified in the 'best' (Table 3) and

marginal DistLMs (Table 4) as significant predictors of D_w, but not D_n or overall rates of denitrification in the present study. Accordingly, simple predictive relationships of N loads and overall rates of denitrification are not possible, especially in oligotrophic estuaries. Ecosystem models should consider factors that enhance rates of D_n when estimating total N removal in estuaries. For example, moderate and comparable rates of total denitrification (up to 118 µmol N m^{-2} h^{-1}; Fig. 4) were documented in the pristine Tautuku River estuary and the relatively eutrophic Avon-Heathcote estuary, despite the different concentrations of inorganic N in the 2 estuaries (Tautuku: <16 µmol l^{-1}, Avon-Heathcote: >60 µmol l^{-1}; Table 1). This is due to the prevalence of D_n in the Tautuku estuary, which is likely influenced by abundant populations of burrow-dwelling amphipods that increase the OPD and enhance diffusive biogeochemical processes.

In the present study, a significant positive relationship was observed between the abundance of macrofauna and the rates of D_n (Fig. 5). Benthic macrofauna stimulate denitrification by increasing the transport of oxygen and NO_3^- from the water column into the sediment through bioturbation and bioirrigation activities (Volkenborn et al. 2010), consuming oxygen during respiration, increasing the availability of organic matter (e.g. mucus, faecal pellets), and excreting NH_4^+ (as an endpoint of protein catabolism), which can be used to support nitrification (Aller 1988). Denitrification usually increases with increasing sediment oxygen consumption because aerobic respiration lowers the concentration of dissolved oxygen in the sediment and increases the demand for alternative electron acceptors such as NO_3^-. The coupling between these 2 processes is also generally attributed to the control of D_n by the decomposition of organic matter that supplies NH_4^+ for nitrification in sediments (Seitzinger 1990). In the present study, *Corophium volutator* was highly abundant at several sites where D_n rates were enhanced (e.g. Tokomairiro estuary mouth, mean 97 400 ind. m^{-2}). This suspension-feeding amphipod can occur at very high densities in estuaries and coasts (maximum abundances of 120 000 ind. m^{-2} were documented in shallow coastal areas in western Sweden; Möller & Rosenberg 1982), where it lives in U-shaped burrows 2–6 cm deep and its continuous irrigation activity can enhance sediment oxygen uptake, D_n, and D_w (by 2-, 3-, and 5-fold, respectively, at densities of 19 800 ind. m^{-2}; Pelegrí et al. 1994). Similarly, the bioturbating crab *Austrohelice crassa* that was recovered in several samples is a common decapod in fine-grained sediments of New Zealand estuaries, where it builds networks of burrows that create increased oxic–suboxic surface areas (Williamson et al. 1999) and may permit nitrification to occur in close proximity to denitrification, thus enhancing the rate of D_n, particularly in muddy sediments (Needham et al. 2010).

The varied life history characteristics of the macrofauna may have contributed to the general trend of lower rates of denitrification in the coarse-grained sandy sediments compared with the fine-grained muddy sediments in this study. The Tautuku and Tokomairiro estuaries had a higher mud content (except at mouth sites) than the other 2 study estuaries and had abundant populations of burrow-dwelling amphipods and spionid polychaetes. By contrast, the Waikouaiti and Avon-Heathcote estuaries had coarse-grained sediments and were dominated by suspension-feeding bivalves, as fine particles can clog the filtering apparatus of suspension feeders. Sediment reworking and irrigation activities of macrofauna can enhance the OPD and alter nutrient fluxes and pathways (Karlson et al. 2007). Furthermore, some macrofauna exhibit trophic trait plasiticity, such as tellinid bivalves, that shift between deposit- and suspension-feeding depending on hydrodynamic conditions (Törnroos et al. 2015), while the functional role of bioturbating crabs as burrow builders is dependent on sediment type (Needham et al. 2010). Therefore, while the sediment grain size influences the types of macrofauna in an area, the functional role of the benthic organisms in nutrient cycling can be dependent on sediment type, making the effect of macrofauna on denitrification often context dependent.

Our findings demonstrate the importance of substratum type as a key driver of denitrification rates in estuaries, with %sand being negatively correlated with rates of D_{tot}, D_n and D_w. Sediment grain size (%sand) was an important explanatory variable explaining differences in rates of denitrification in the New Zealand estuaries in all the models that considered combinations of environmental predictors simultaneously and models that tested predictors individually (Tables 3 & 4). Further, denitrification rates were lowest at the mouth sites in each estuary and at the Waikouaiti River estuary, which had the highest %sand among the study estuaries, while rates of denitrification were greatest at the middle and upstream sites in the Tokomairiro River estuary, which was dominated by fine-grained sediment. Similarly, studies from freshwater rivers and streams or continental shelf sediments have found higher rates of denitrification in fine-grained sediment com-

pared with coarse-grained sediment (Pattinson et al. 1998, Sundbäck & Miles 2000, Inwood et al. 2005, Vance-Harris & Ingall 2005, Solomon et al. 2009, Deutsch et al. 2010). There are 3 possible explanations for lower rates of denitrification at sandy sites compared with sites dominated by fine-grained mud. Firstly, the population sizes of the nitrifying and denitrifying bacteria could be limited in the sandy sediment because of competition with larger populations of heterotrophic bacteria for space (Henriksen & Kemp 1988). Less surface area is available for bacteria to colonize in larger substrata compared with smaller substrata, thus denitrifying bacteria may reach their maximum carrying capacity in sandy sediment quicker than in muddy sediment. Secondly, nitrification could have been inhibited in the sandy sediment because of the deeper penetration of light in sandy sediment compared with muddy sediment (Fenchel & Straarup 1971) and because nitrifying bacteria are inhibited even at low light intensities (Olson 1981, Guerrero & Jones 1996). Thirdly, sandy sediments are highly permeable compared with muddy sediments, meaning that solute exchange is also mediated by advection-driven sediment pressure gradients (Burdige 2006). In sandy sediments, advective flushing delivers oxygenated bottom water to different areas of the sediment matrix, where it comes in contact with suboxic porewater and potentially stimulates D_w in these places (Cook et al. 2006). However, core incubations in a laboratory may limit advective flushing and hence underestimate denitrification rates of sandy sediments relative to muddy sediments. In the present study, this was partially overcome using intact sediment cores with benthic infauna, which can induce pressure gradients in the sediment that move solutes (Woodin et al. 2012). Moreover, one of the assumptions of the IPM is that there is uniform mixing of the *in situ* NO_3^- and labelled $^{15}NO_3^-$, which can be negatively influenced by advection, and hence the experimental set-up was based on a diffusive exchange model.

In addition to sediment grain size, the 'best' AIC_c models identified OPD and ammonia concentrations as significant predictors of D_n and D_w, respectively (Table 3). OPD was positively related to rates of D_n in the present study, which supports results of previous studies in subtidal marine sediments (Jensen et al. 1996) and in freshwater sediment microcosms (Jensen et al. 1994). Because D_n occurs at the oxic–anoxic interface in sediments, the presence of oxygen in the surface sediments from the overlying water column or an increase in the surface area of oxic and anoxic microenvironments around macrofaunal burrows (Pelegrí et al. 1994, Karlson et al. 2007) increases the sites for possible D_n. In contrast, high concentrations of oxygen in surface sediments increase the diffusional distance that NO_3^- must travel from the water column to reach the suboxic denitrification zone. This often results in reduced efficiency of D_w (Rysgaard et al. 1994).

Sedimentary organic carbon content was also a significant driver and positively related to rates of denitrification (D_{tot}, D_n, and D_w) in the marginal tests (Table 4), consistent with studies in other aquatic systems (Jensen et al. 1988, Yoon & Benner 1992, Barnes & Owens 1999, Dong et al. 2000, Arango & Tank 2008, Deutsch et al. 2010). The sediment oxygen demand data demonstrate that there are high rates of oxygen consumption in most sites (Fig. 3), which indicates bacterial breakdown of organic carbon in the sediments. Organic carbon can stimulate denitrification directly by providing substrate for bacterial growth and indirectly by supplying NH_4^+ for nitrification and by consuming oxygen during mineralization (Kelly & Nixon 1984). In the New Zealand study estuaries, organic matter was available to the denitrifying bacteria from detrital seagrass and macroalgae as well as microphytes (Savage et al. 2012). Further, chl *a* concentrations in the top 0–2 cm of the sediments (a proxy of microphyte biomass) were positively correlated with rates of overall denitrification and explained 23% of the variance in D_n rates across all sites when predictors are considered individually. Photosynthesis by microphytes can release oxygen into the sediments and increase the depth interval in which nitrification could occur, if the bacteria are not limited by competition with benthic microphytes for DIN (Risgaard-Petersen et al. 1994, Risgaard-Petersen 2003).

Performing the denitrification incubations under illuminated conditions may have enhanced rates of D_n as photosynthesis by microphytes could increase the OPD. A study of photosynthetic microphytes at the sediment surface shows that they can cause large diurnal variations in the sediment OPD, and this can have a marked effect on the rates of nitrification and denitrification (Risgaard-Petersen et al. 1994). At night, when microbes and macrofauna in sediment are consuming oxygen and oxygen production via photosynthesis is inhibited, the vertical extent of the sediment oxic zone is narrow and the rate of D_w is generally much greater than the rate of D_n (Risgaard-Petersen et al. 1994). In contrast, during the daytime, when oxygen is produced by microphytes via photosynthesis and released into the surrounding sediments, the vertical extent of the sediment oxic zone

(and therefore also the depth interval in which nitrification can occur) is thick and the rate of D_n is generally much greater than the rate of D_w (Risgaard-Petersen et al. 1994). However, in the present study, chl *a* was not included in the 'best' AIC_c models for D_n when all variables are considered together (Table 3). Moreover, whole-core oxygen flux incubations at each study site demonstrated that oxygen uptake by the sediments (146–1597 µmol m^{-2} h^{-1}) was much higher than oxygen release, and the low chl *a* concentrations in the surface sediment (Table 1) indicate a high oxygen demand by these sediments and low microphyte primary production during the experiment. Consequently, the effect of performing the denitrification measurements under illuminated conditions in the present study was likely minimal. Further, denitrification rates at all sites were measured under the same illuminated conditions, supporting the finding that D_n is an important N removal process relative to D_w in New Zealand's oligotrophic estuaries.

In the New Zealand study estuaries, N_2O formed at much smaller concentrations than N_2, with N_2 comprising >98% of the gases produced, except at AH5, which had relatively high DIN concentrations (Fig. 4D). The majority of the N_2O produced was likely a consequence of incomplete reduction of NO_3^-, but it cannot be ruled out that some of the N_2O may have been produced during nitrification or dissimilatory nitrate reduction to ammonium. The ratio of N_2O:N_2 produced increased with increasing DIN concentration in the water column; however, this finding should be treated with caution because the highest ratio, which occurred at AH5 (N_2O:N_2: 11.20%, DIN: 140 µmol l^{-1}), largely determined this trend. Seitzinger and Kroeze (1998) suggested that the ratio of N_2O:N_2 produced from sediment denitrification is generally within the range of 0.1 and 0.5%, but can be as high as 6% in heavily eutrophic systems. Dong et al. (2006) found that the ratio of N_2O:N_2 was 2.6% in the oligotrophic Conwy Estuary, 1.1% in the nutrient-enriched Humber Estuary, and 3.3% in the highly eutrophic Colne Estuary. The higher N_2O:N_2 ratio is undesirable because N_2O is a potent greenhouse gas and is linked to many environmental and human health problems (Badr & Probert 1993, Fields 2004). Reducing the input of DIN (particularly NH_4^+) to the estuaries may be a successful means for decreasing the ratio of N_2O:N_2.

The focus of the present study was to quantify spatial variation in rates of denitrification and the environmental drivers across and among estuaries, rather than investigate seasonal variation in N removal rates. Sampling was therefore conducted in one season only for most study estuaries. However, temporal sampling at the Avon-Heathcote estuary showed no seasonal differences in the rates of denitrification (C. Gongol unpubl. data). The research presented here was conducted during the southern hemisphere spring to coincide with elevated concentrations of water column N following winter rains and before macroalgae or microphytes compete with denitrifying bacteria for N, and accordingly are considered estimates of maximum N removal rates.

Implications of results

Nutrient inputs to aquatic ecosystems are increasing worldwide, causing shifts in biological community structure and trophic interactions (Fox et al. 2009) and affecting ecosystem functioning in many estuaries (Norkko et al. 2013). While nutrient budgets have been developed for New Zealand estuaries (Heggie & Savage 2009), there are no published studies that quantify the magnitude of N removal and the factors that influence this crucial ecosystem service in New Zealand estuaries. Using the IPM, we present the first measured rates of denitrification for New Zealand estuaries and provide useful input data for biogeochemical models. Our data support findings from denitrification research globally that show N removal rates via D_w are positively related to water column DIN concentrations (Seitzinger 1988) while D_n is related to OPD, which, in turn, is partly mediated by the benthic macrofauna. Sediment grain size was a key environmental factor related to variation in rates of denitrification across and among the 4 study estuaries. The influence of sediment grain size on biogeochemical processes has important implications for modelling future changes in N cycling, as inputs of fine-grained sediments to estuaries are predicted to increase with changes in land use and increasing development in catchments in New Zealand and globally (Lohrer et al. 2004). An increase in mud content will also cause shifts in macrobenthic community composition (Robertson et al. 2015), the functional role of organisms (Needham et al. 2010), and behaviours that influence porewater hydraulics (Woodin et al. 2012), which can further affect denitrification rates indirectly. Given the importance of D_n in New Zealand's oligotrophic estuaries, there is an urgent need for further empirical data on the effects of increasing mud content on denitrification rates, both directly through altered biophysical processes and indirectly through shifts in macrofaunal community

composition and their functional traits. Furthermore, as estuaries are progressively exposed to multiple stressors, research on the synergistic effects of increasing mud and elevated nutrient inputs on denitrification is needed to better inform biogeochemical models of N cycling in estuaries.

Acknowledgements. The authors gratefully acknowledge the University of Otago for PBRF funding and a postgraduate scholarship that made the study possible. The National Institute of Water and Atmospheric (NIWA) are thanked for funding that facilitated the write-up of this research as a manuscript. We thank Dr. John Zeldis and staff at NIWA, Christchurch, for access to their laboratories for the Avon-Heathcote work. The staff at the Portobello Marine Laboratory are thanked for facilities and logistical support for the manufacture of the experimental equipment. We thank the editor and reviewers for constructive comments, which have greatly improved the manuscript.

LITERATURE CITED

Aller RC (1988) Benthic fauna and biogeochemical processes in marine sediments: the role of burrow structures. In: Blackburn T, Sørenson J (eds) Nitrogen cycling in coastal marine environments. John Wiley & Sons, Chichester, p 301–338

Anderson MJ, Gorley RN, Clarke KR (2008) PERMANOVA+ for PRIMER. Guide to software and statistical methods. PRIMER-E, Plymouth

Arango CP, Tank JL (2008) Land use influences the spatiotemporal controls on nitrification and denitrification in headwater streams. J N Am Benthol Soc 27:90–107

Badr O, Probert SD (1993) Environmental impacts of atmospheric nitrous-oxide. Appl Energy 44:197–231

Barnes J, Owens NJP (1999) Denitrification and nitrous oxide concentrations in the Humber estuary, UK, and adjacent coastal zones. Mar Pollut Bull 37:247–260

Berg P, Risgaard-Petersen N, Rysgaard S (1998) Interpretation of measured concentration profiles in sediment pore water. Limnol Oceanogr 43:1500–1510

Bolton-Ritchie L, Main M (2005) Nutrient water quality Avon-Heathcote Estuary/Ihutai: inputs, concentrations and potential effects. Environment Canterbury report

Broecker WS, Peng TH (1974) Gas exchange rates between air and sea. Tellus 26:21–35

Burdige DJ (2006) Geochemistry of marine sediments. Princeton University Press, Princeton, NJ

Cabrita MT, Brotas V (2000) Seasonal variation in denitrification and dissolved nitrogen fluxes in intertidal sediments of the Tagus estuary, Portugal. Mar Ecol Prog Ser 202:51–65

Cook PLM, Revill AT, Butler ECV, Eyre BD (2004) Carbon and nitrogen cycling on intertidal mudflats of a temperate Australian estuary. II. Nitrogen cycling. Mar Ecol Prog Ser 280:39–54

Cook PL, Wenzhöfer F, Rysgaard S, Galaktionov OS and others (2006) Quantification of denitrification in permeable sediments: Insights from a two-dimensional simulation analysis and experimental data. Limnol Oceanogr 4: 294–307

Cornwell J, Kemp WM, Kana T (1999) Denitrification in coastal ecosystems: methods, environmental controls, and ecosystem level controls: a review. Aquat Ecol 33:41–54

Dalsgaard T, Nielsen LP, Brotas V, Viaroli P and others (2000) Protocol handbook for NICE – Nitrogen Cycling in Estuaries: a project under the EU research programme: Marine Science and Tecnology (MAST III). National Environmental Research Institute, Silkeborg

Dettmann EH (2001) Effect of water residence time on annual export and denitrification in estuaries: a model analysis. Estuaries 24:481–490

Deutsch B, Forster S, Wilhelm M, Dippner J, Voss M (2010) Denitrification in sediments as a major nitrogen sink in the Baltic Sea: an extrapolation using sediment characteristics. Biogeosciences 7:2487–2521

Dong LF, Thornton DCO, Nedwell DB, Underwood GJC (2000) Denitrification in sediments of the River Colne estuary, England. Mar Ecol Prog Ser 203:109–122

Dong LF, Nedwell DB, Stott A (2006) Sources of nitrogen used for denitrification and nitrous oxide formation in sediments of the hypernutrified Colne, the nutrified Humber, and the oligotrophic Conwy estuaries, United Kingdom. Limnol Oceanogr 51:545–557

Eyre BD, Rysgaard S, Dalsgaard T, Christensen PB (2002) Comparison of isotope pairing and N_2:Ar methods for measuring sediment denitrification–assumptions, modifications, and implications. Estuaries 25(6A):1077–1087

Fenchel T, Straarup BJ (1971) Vertical distribution of photosynthetic pigments and penetration of light in marine sediments. Oikos 22:172–182

Fields S (2004) Global nitrogen: cycling out of control. Environ Health Perspect 112:A556–A563

Fox SE, Teichberg M, Olsen YS, Heffner L, Valiela I (2009) Restructuring of benthic communities in eutrophic estuaries: lower abundance of prey leads to trophic shifts from omnivory to grazing. Mar Ecol Prog Ser 380:43–57

Glud RN (2008) Oxygen dynamics of marine sediments. Mar Biol Res 4:243–289

Gran V, Pitkänen H (1999) Denitrification in estuarine sediments in the eastern Gulf of Finland, Baltic Sea. Hydrobiologia 393:107–115

Groffman PM, Altabet MA, Bohlke JK, Butterbach-Bahl K and others (2006) Methods for measuring denitrification: diverse approaches to a difficult problem. Ecol Appl 16: 2091–2122

Guerrero MA, Jones RD (1996) Photoinhibition of marine nitrifying bacteria. I. Wavelength-dependent response. Mar Ecol Prog Ser 141:183–192

Hamilton SK, Ostrom NE (2007) Measurement of the stable isotope ratio of dissolved N_2 in N-15 tracer experiments. Limnol Oceanogr Methods 5:233–240

Heggie K, Savage C (2009) Nitrogen yields from New Zealand coastal catchments to receiving estuaries. NZ J Mar Freshw Res 43:1039–1052

Henriksen K, Kemp WM (1988) Nitrification in estuarine and coastal marine sediments. In: Blackburn T, Sørenson J (eds) Nitrogen cycling in coastal marine environments. John Wiley & Sons, Chichester, p 207–249

Inwood SE, Tank JL, Bernot MJ (2005) Patterns of denitrification associated with land use in 9 midwestern headwater streams. J N Am Benthol Soc 24:227–245

Jensen MH, Andersen TK, Sorensen J (1988) Denitrification in coastal bay sediment: regional and seasonal variation in Aarhus Bight, Denmark. Mar Ecol Prog Ser 48: 155–162

Jensen K, Sloth NP, Risgaard-Petersen N, Rysgaard S, Revs-

bech NP (1994) Estimation of nitrification and denitrification from microprofiles of oxygen and nitrate in model sediment systems. Appl Environ Microbiol 60:2094–2100

Jensen KM, Jensen MH, Kristensen E (1996) Nitrification and denitrification in Wadden Sea sediments (Konigshafen, Island of Sylt, Germany) as measured by nitrogen isotope pairing and isotope dilution. Aquat Microb Ecol 11:181–191

Jones MB, Marsden ID (2005) Life in the estuary, illustrated guide and ecology. Canterbury University Press, Christchurch

Karlson K, Bonsdorff E, Rosenberg R (2007) The impact of benthic macrofauna for nutrient fluxes from Baltic Sea sediments. Ambio 36:161–167

Kelly JR, Nixon SW (1984) Experimental studies of the effect of organic deposition on the metabolism of a coastal marine bottom community. Mar Ecol Prog Ser 17:157–169

Lewis DW, McConchie D (1994) Analytical sedimentology. Chapman & Hall, New York, NY

Li YH, Gregory S (1974) Diffusion of ions in sea water and in deep-sea sediments. Geochim Cosmochim Acta 38: 703–714

Lohrer AM, Thrush SF, Hewitt JE, Berkenbusch K, Ahrens M, Cummings VJ (2004) Terrestrially derived sediment: response of marine macrobenthic communities to thin terrigenous deposits. Mar Ecol Prog Ser 273:121–138

Lohse L, Kloosterhuis HT, van Raaphorst W, Helder W (1996) Denitrification rates as measured by the isotope pairing method and by the acetylene inhibition technique in continental shelf sediments of the North Sea. Mar Ecol Prog Ser 132:169–179

McLay CL (1976) An inventory of the status and origin of New Zealand estuarine systems. Proc NZ Ecol Soc 23: 8–26

Möller P, Rosenberg R (1982) Production and abundance of the amphipod *Corophium volutator* on the west coast of Sweden. Neth J Sea Res 16:127–140

Needham HR, Pilditch CA, Lohrer AM, Thrush SF (2010) Habitat dependence in the functional traits of *Austrohelice crassa*, a key bioturbating species. Mar Ecol Prog Ser 414:179–193

Nielsen LP (1992) Denitrification in sediment determined from nitrogen isotope pairing. FEMS Microbiol Ecol 86: 357–362

Norkko A, Vilnas A, Norkko J, Valanko S, Pilditch C (2013) Size matters: implications of the loss of large individuals for ecosystem functioning. Sci Rep 3:2646

Ogilvie B, Nedwell DB, Harrison RM, Robinson A, Stage A (1997) High nitrate, muddy estuaries as nitrogen sinks: the nitrogen budget of the River Colne estuary (United Kingdom). Mar Ecol Prog Ser 150:217–228

Olson RJ (1981) Differential photoinhibition of marine nitrifying bacteria: a possible mechanism for the formation of primary nitrite maximum. J Mar Res 39:227–238

ORC (Otago Regional Council) (2000) North and coastal Otago River catchments monitoring report. Otago Regional Council, Dunedin

Pattinson SN, Garcia-Ruiz R, Whitton BA (1998) Spatial and seasonal variation in denitrification in the Swale-Ouse system, a river continuum. Sci Total Environ 210–211: 289–305

Pelegrí SP, Nielsen LP, Blackburn TH (1994) Denitrification in estuarine sediment stimulated by the irrigation activity of the amphipod *Corophium volutator*. Mar Ecol Prog Ser 105:285–290

Risgaard-Petersen N (2003) Coupled nitrification–denitrification in autotrophic and heterotrophic estuarine sediments: on the influence of benthic microalgae. Limnol Oceanogr 48:93–105

Risgaard-Petersen N, Rysgaard S, Nielsen LP, Revsbech NP (1994) Diurnal variation of denitrification and nitrification in sediments colonized by benthic microphytes. Limnol Oceanogr 39:573–579

Robertson BP, Gardner JPA, Savage C (2015) Macrobenthic-mud relations strengthen the foundation for benthic index development: a case study from shallow, temperate New Zealand estuaries. Ecol Indic 58:161–174

Rysgaard S, Risgaard-Petersen N, Nielsen LP, Revsbech NP (1993) Nitrification and denitrification in lake and estuarine sediments measured by the ^{15}N dilution technique and isotope pairing. Appl Environ Microbiol 59:2093–2098

Rysgaard S, Risgaard-Petersen N, Sloth NP, Jensen K, Nielsen LP (1994) Oxygen regulation of nitrification and denitrification in sediments. Limnol Oceanogr 39: 1643–1652

Rysgaard S, Christensen PB, Nielsen LP (1995) Seasonal variation in nitrification and denitrification in estuarine sediment colonized by benthic microalgae and bioturbating infauna. Mar Ecol Prog Ser 126:111–121

Savage C, Thrush SF, Lohrer AM, Hewitt JE (2012) Ecosystem services transcend boundaries: estuaries provide resource subsidies and influence functional diversity in coastal benthic communities. PLOS ONE 7:e42708

Seitzinger SP (1987) Nitrogen biogeochemistry in an unpolluted estuary: the importance of benthic denitrification. Mar Ecol Prog Ser 41:177–186

Seitzinger SP (1988) Denitrification in fresh-water and coastal marine ecosystems: ecological and geochemical significance. Limnol Oceanogr 33:702–724

Seitzinger SP (1990) Denitrification in aquatic sediments. In: NP Revsbech, J Sørensen (eds) Denitrification in soil and sediment, FEMS Symposium no. 56. Plenum, New York, NY, p 301–322

Seitzinger SP, Kroeze C (1998) Global distribution of nitrous oxide production and N inputs in freshwater and coastal marine ecosystems. Global Biogeochem Cycles 12: 93–113

Seitzinger S, Harrison JA, Bohlke JK, Bouwman AF and others (2006) Denitrification across landscapes and waterscapes: a synthesis. Ecol Appl 16:2064–2090

Solomon CT, Hotchkiss ER, Moslemi JM, Ulseth AJ, Stanley EH, Hall RO Jr, Flecker AS (2009) Sediment size and nutrients regulate denitrification in a tropical stream. J N Am Benthol Soc 28:480–490

Sundbäck K, Miles A (2000) Balance between denitrification and microalgal incorporation of nitrogen in microtidal sediments, NE Kattegat. Aquat Microb Ecol 22:291–300

Sundbäck K, Miles A, Göransson E (2000) Nitrogen fluxes, denitrification and the role of microphytobenthos in microbial shallow-water sediments: an annual study. Mar Ecol Prog Ser 200:59–76

Symonds MRE, Moussalli A (2011) A brief guide to model selection, multimodel inference and model averaging in behavioural ecology using Akaike's information criterion. Behav Ecol Sociobiol 65:13–21

Törnroos A, Nordström MC, Aarnio K, Bonsdorff E (2015) Environmental context and trophic trait plasticity in a key species, the tellinid clam *Macoma balthica* L. J Exp Mar Biol Ecol 472:32–40

Tuominen L, Heinänen A, Kuparinen J, Nielsen LP (1998)

Spatial and temporal variability of denitrification in the sediments of the northern Baltic Proper. Mar Ecol Prog Ser 172:13–24

Ullman WJ, Aller RC (1982) Diffusion coefficients in nearshore marine sediments. Limnol Oceanogr 27:552–556

Usui T, Koike I, Ogura N (2001) N_2O production, nitrification and denitrification in an estuarine sediment. Estuar Coast Shelf Sci 52:769–781

Vance-Harris C, Ingall E (2005) Denitrification pathways and rates in the sandy sediments of the Georgia continental shelf, USA. Geochem Trans 6:12–18

Vanderborght JP, Billen G (1975) Vertical distribution of nitrate concentration in interstitial water of marine sediments with nitrification and denitrification. Limnol Oceanogr 20:953–961

Volkenborn N, Polerecky L, Wethey DS, Woodin SA (2010) Oscillatory porewater bioadvection in marine sediments induced by hydraulic activities of *Arenicola marina*. Limnol Oceanogr 55:1231–1247

Weiss RF (1970) Solubility of nitrogen, oxygen and argon in water and seawater. Deep-Sea Res 17:721–735

Weiss RF, Price BA (1980) Nitrous oxide solubility in water and seawater. Mar Chem 8:347–359

Williamson RB, Wilcock RJ, Wise BE, Pickmere SE (1999) Effect of burrowing by the crab *Helice crassa* on chemistry of intertidal muddy sediments. Environ Toxicol Chem 18:2078–2086

Woodin SA, Wethey DS, Hewitt JE, Thrush SF (2012) Small scale terrestrial clay deposits on intertidal sandflats: Behavioral changes and productivity reduction. J Exp Mar Biol Ecol 413:184–191

Yoon WB, Benner R (1992) Denitrification and oxygen consumption in sediments of two south Texas estuaries. Mar Ecol Prog Ser 90:157–167

Editorial responsibility: William Kemp, Cambridge, Maryland, USA

Submitted: March 15, 2016; Accepted: August 4, 2016
Proofs received from author(s): September 5, 2016